BAJOPAS Volume 10 Number 1 June, 2017

http://dx.doi.org/10.4314/bajopas.v10i1.26

Bayero Journal of Pure and Applied Sciences, 10(1): 183 - 190
Received: December, 2016
Accepted: April, 2017
ISSN 2006 – 6996

MOLECULAR DYNAMICS OF A PROGUANIL DERIVATIVE

*** Muhammad, A.[1], Taura, L .S.[1] and Ndikilar, C.E.[2]**
[1]Department of Physics, Sule Lamido University Kafin-Hausa, Jigawa State
[2]Department of Physics, Federal University Dutse, Jigawa State
[*]Correspondence author:aminumuhammad1427@gmail.com (08130661127)

ABSTRACT
Proguanil is a prophylactic antimalarial drug that is very effective against sporozoites and works by stopping the malaria parasites from reproducing inside the red blood cells. In this work, the molecular dynamics of a derivative of Proguanil is studied. A Hydrogen atom at position 3 on the benzene ring of the molecule of Proguanil is substituted by chlorine atom to give the desired derivative. The molecular geometries of Proguanil derivative are studied using ab-initio Quantum chemical calculations at the Restricted Hatree-Fock (RHF) level of theory using the basis sets 6-31G(d,p) and 6-31++G. Also, Density Functional Theory (DFT) calculations at B3LYP with 6-31G(d,p) and 6-31++G basis sets were carried out for inclusion of electron correlation. The dipole moments, thermal energies, quadrupole moment, polarizibility and optimized bond length computations for the molecule are obtained. The dipole moment of the Proguanil's derivative at both levels of theory is less than that obtained for original malaria drug Proguanil. This indicates that the derivative Proguanil responds significantly more than Proguanil to an applied electric field. The Infra Red (IR) and Raman vibrational frequencies are vividly examined and the most intense IR and Raman frequencies are identified. The computation was performed using Gaussian 03W software.
Keywords: Proguanil, Density Functional Theory, Restricted Hartree Fock, Gaussian

INTRODUCTION

Malaria has been well known to be the most important parasitic infection of man in tropical regions over the years. Malaria has had great impact on the history of humanity as it is one of the oldest known diseases to mankind. Currently, it is estimated that about 2 billion people are at risk of malaria resulting in about 500 million cases annually and one million deaths. The majority of malaria cases exist in developing countries of the tropics and sub-tropics with the majority of casualties being among children. Malaria thus represents a significant impediment to the socio economic development of these tropical countries (Singh, 2002).

There is a limited number of drugs which can be used to treat or prevent malaria. The most widely used are Quinine and it is derivatives (Chloroquine, Primaquine, Mefloquine), and the antifolate drugs (Proguanil, Chloproguanil, Clociguanil, BRL 6231 (WR99210), Pryrimethamine, Sulfadoxine, Sulfalene, Dapsone and their combination with other drugs (Atovaqone and Proguanil Hydrochloride, Pryrimethamine/Sulfadoxine, Pryrimethamine/ Sulfadoxine/Artesunate) (Schwarz, 2002).

Pyrimethamine was first developed in 1952 by Crud, Davy and Rose from the synthesis of the antifolate drug Paludrine or from Proguanil (chlorguamide Hydrochloride) (Snow, 2005). It is an antiparasitic compound and a hydrofolate reductase inhibitor (Sachs & Malaney, 2002). It is a Folic acid antagonist and the rationale for its therapeutic action is based on the differential requirement between host and parasite for nucleic acid precursors involved in growth. Pyrimethamine possesses blood schizonticidal and some tissue schizonticidal activity against malaria parasite in human (Singh *et al* 2002). Its inhibition activity leads to either killing a pathogenic organism (malaria parasite) or to modify some aspects of metabolism of the body that are functioning dormally. Daraprim interferes with the biosynthesis of the parasite.

Pyrimethamine on the other hand, inhibits the dihydrofolate reductase of plasmodia and thereby blocking the biosynthesis of purine and pyrimidine which are essential for DNA synthesis and cell multiplication (Chifu, 2014). This leads to failure of nuclear division at the time of schizont formation in the erythrocytes and liver. Daraprim is a weak basic drug and sparingly soluble in water.

For almost three quarters of a century, Daraprim is used as one of the anti malaria resistance drug in some countries (places) where Quinine and its derivatives failed to treat malaria. It is recommended for patients infected in areas where susceptible plasmodia exist (Geh, 2015). Although the drug has antimalarial activity when used alone, parasitological resistance can develop rapidly(Schwarz, 2002). When used in combination, it produces a synergistic effect on the parasite and can be effective even in the presence of resistance to individual component. It is usually used in combination with Sulfadoxine.

Proguanil is a prophylactic antimalarial drug that is very effective against sporozoites and works by stopping the malaria parasites from reproducing inside the red blood cells (Schwarz, 2002).

In an earlier article (Chifu, 2014) a thorough study of the molecular dynamics of this molecule was carried out in gas phase at Restricted Hartree Fock (RHF) and Density Functional Theory (DFT) levels of theory. In this research article; we provide a systematic study of a derivative of Proguanil, 3-Chloroproguanil and compare the molecular dynamics of this molecule to that of Proguanil

Computational Methodology

The Gaussian software is used in this study. Mainly, the Gaussian program is characterized by using different basis sets. This is the mathematical representation of the molecular orbital within the molecules and can be interpreted as restricting each electron to a particular region of space. This implies that larger basis sets impose fewer constraints on electrons and more accurately approximate exact molecular orbitals. The optimized structure and molecular dynamics of the molecule is obtained. The molecular structures and geometries of the malaria drug, 3-Chloro Proguanil is completely optimized using ab- initio quantum mechanical calculations at the Restricted Hartree-Fock (RHF) level of theory using the basis sets 6-31++G and 6-31G(d,p). The structures are further refined using Density Functional Theory (DFT) which is a cost effective method for inclusion of electron correlations with the three parameter density functional generally known as Becke3LYP (B3LYP) (Becke,1993), (Becke,1988) &(Lee et al,1988) using the same basis sets. At the first step, geometry optimizations are carried out, then later the Infra Red (IR) and Raman frequencies are calculated using the Hessian which is the matrix of second derivatives of the energy with respect to geometry.

The energies of the highest occupied molecular orbital (HOMO) and lowest unoccupied molecular orbital (LUMO) are computed. Also, total energies, dipole and quadrupole moments are computed. A detailed analysis of the IR and Raman active vibrational frequencies is carried out to determine the most intense frequencies and their descriptions. All computations in this work were modeled in gas phase.

RESULTS AND DISCUSSION

Optimized Molecular Structures

Geometry optimizations usually attempt to locate minima on the potential energy surface, thereby predicting equilibrium structures of molecular systems (Frisch *et al* 2004). At the minima, the first derivative of the energy (gradient) is zero. Since the gradient is the negative of the forces, the forces are also zero at such a point (stationary point). In Gaussian, a geometry optimization begins at the molecular structure specified at the input and steps along the potential energy surface. It computes the energy and the gradient at that point and determines which direction to make the next step. The gradient indicates the direction along the surface in which the energy decreases most rapidly from the current point as well as the steepness of that slope. Atoms in the molecule are numbered according to their order in the molecule specification section of the input.

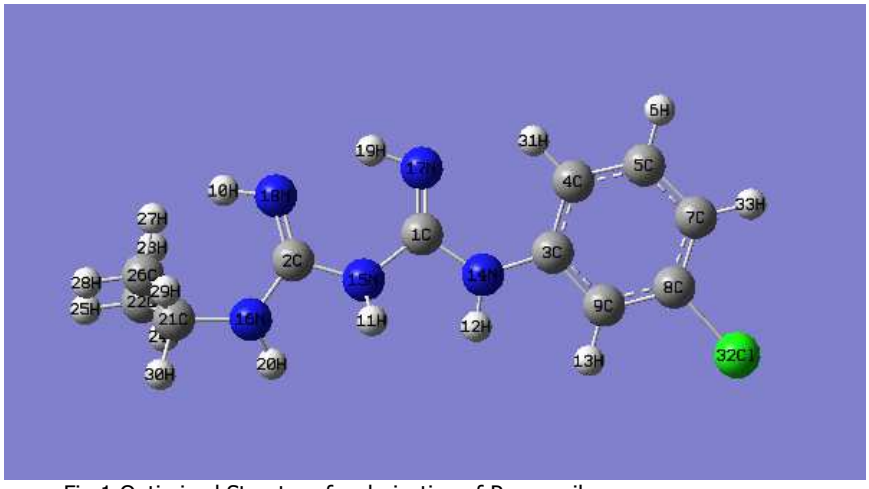

Fig.1 Optimized Structure for derivative of Proguanil

Table 1: Optimized Bond Lengths (Å) for derivative of Proguanil

Geometrical Parameter	RHF 6-31++G	RHF 6-31G(d,p)	B3LYP 6-31++G	B3LYP 6-31G(d,p)
R(1,14)	1.3914	1.3879	1.8892	1.8461
R(1,15)	1.4084	1.4084	1.7313	1.6985
R(1,17)	1.2463	1.2608	1.897	1.8491
R(2,15)	1.3931	1.3909	1.8942	1.8522
R(2,16)	1.3805	1.3767	1.7367	1.6989
R(2,18)	1.2588	1.2742	1.8808	1.8444
R(3,4)	1.3923	1.3951	1.4041	1.4019
R(3,9)	1.3933	1.399	1.4054	1.4044
R(3,14)	1.4009	1.4018	1.8881	1.8428
R(4,5)	1.3832	1.3887	1.4023	1.3952
R(4,31)	1.0683	1.0661	1.0857	1.0862
R(5,6)	1.0757	1.073	1.0835	1.0841
R(5,7)	1.3847	1.3882	1.3925	1.3928
R(7,8)	1.380	1.3795	1.3948	1.396
R(7,33)	1.073	1.0704	1.8259	1.7567
R(8,9)	1.3793	1.3758	1.4003	1.3923
R(8,32)	1.7469	1.8129	1.0837	1.0843
R(9,13)	1.075	1.0726	1.0856	1.0859
R(10,18)	0.9961	0.9977	1.4614	1.4346
R(11,15)	0.995	0.9934	1.4512	1.4248
R(12,14)	0.9936	0.9924	1.4519	1.4247
R(16,20)	0.9952	0.9931	1.4595	1.4323
R(16,21)	1.4634	1.4701	1.4493	1.4225
R(17,19)	1.0009	1.0023	1.5346	1.5324
R(21,22)	1.533	1.5346	1.5349	1.5332
R(21,26)	1.5296	1.5322	1.0998	1.0996
R(21,30)	1.0853	1.0844	1.9618	1.9034
R(22,23)	1.0837	1.0826	1.0966	1.0951
R(22,24)	1.0853	1.0833	1.0958	1.0941
R(22,25)	1.0855	1.0847	1.099	1.0968
R(26,27)	1.0829	1.0816	1.0969	1.0956
R(26,28)	1.0851	1.0843	1.098	1.0958
R(26,29)	1.0838	1.0828	1.0953	1.0941

Table 2: Optimized Bond Angles (°) for derivative of Proguanil

Geometrical Parameter	RHF 6-31++G	RHF 6-31G(d,p)	B3LYP 6-31++G	B3LYP 6-31G(d,p)
A(14,1,15)	107.9224	109.4692	120.725	120.7868
A(14,1,17)	123.7486	123.354	112.823	112.3253
A(15,1,17)	128.329	127.1768	126.4508	126.8837
A(15,2,16)	109.5284	111.4411	114.0578	112.4651
A(15,2,18)	121.4075	120.4315	122.6837	123.8422
A(16,2,18)	129.054	128.1239	123.1598	123.6045
A(4,3,9)	119.1722	119.114	119.1825	118.6146
A(4,3,14)	124.1357	124.5217	118.1155	118.1911
A(9,3,14)	116.6305	116.3631	122.6868	123.1752
A(3,4,5)	119.3522	119.4315	120.769	121.1148
A(3,4,31)	119.9025	119.4936	120.0082	119.8006
A(5,4,31)	120.7285	121.0689	119.2228	119.0842
A(4,5,6)	118.7557	118.8483	120.7705	120.8575
A(4,5,7)	122.0827	121.8793	118.6191	118.9427
A(6,5,7)	119.1615	119.2711	120.6101	120.1991
A(5,7,8)	117.6869	117.518	122.0317	121.2625
A(5,7,33)	121.565	121.589	119.0325	119.4356
A(8,7,33)	120.7479	120.8927	118.9355	119.3016
A(7,8,9)	121.7387	122.3624	118.7275	119.0879
A(7,8,32)	119.541	119.2025	120.4899	120.0849
A(9,8,32)	118.7202	118.4347	120.7825	120.8271
A(3,9,8)	119.9671	119.6925	120.6684	120.975
A(3,9,13)	120.558	120.6276	120.3011	119.9998
A(8,9,13)	119.4748	119.679	119.029	119.0247
A(1,14,3)	127.8552	129.1023	112.0543	111.8219
A(1,14,12)	113.9375	115.9867	109.3755	108.6522

Table 2 continue

A(3,14,12)	113.6723	114.5644	114.1404	115.2977
A(1,15,2)	126.7722	126.9839	108.8662	108.0109
A(1,15,11)	113.9248	116.0372	110.8043	111.5404
A(2,15,11)	113.876	115.9096	100.9323	100.6722
A(2,16,20)	112.9761	116.4117	111.044	111.1592
A(2,16,21)	126.282	127.5338	112.0005	111.8983
A(20,16,21)	113.4494	115.5222	110.0253	110.3023
A(1,17,19)	110.8786	114.3865	108.3533	108.1491
A(2,18,10)	112.8647	116.6101	107.515	107.3999
A(16,21,22)	114.1193	113.332	107.7391	107.7576
A(16,21,26)	112.1535	112.3535	111.2659	111.3848
A(16,21,30)	103.4092	103.5754	109.8509	110.0836
A(22,21,26)	113.1635	112.8366	111.9632	111.9512
A(22,21,30)	106.7585	106.9966	107.2475	107.1586
A(26,21,30)	106.2633	106.9435	108.2612	108.0078
A(21,22,23)	112.8483	112.6128	108.0836	108.0729
A(21,22,24)	110.5714	110.5767	104.1645	105.2256
A(21,22,25)	109.9007	109.8539	96.565	96.8602
A(23,22,24)	107.7179	107.9266	97.8228	98.4242
A(23,22,25)	107.6552	107.5062	97.3433	97.5415
A(24,22,25)	107.9784	108.2151	102.8386	104.2657
A(21,26,27)	113.0115	112.6025	96.4195	96.7983
A(21,26,28)	109.5327	109.6437	97.79	98.3789
(21,26,29)	110.1776	110.3975	97.5946	98.2504
A(27,26,28)	107.6469	107.7488	97.9839	98.2848
A(27,26,29)	107.9441	107.9973	103.0678	104.01
A(28,26,29)	108.3932	108.3214	95.7642	96.0287

Dipole Moments

The dipole moment is the first derivative of the energy with respect to an applied electric field. It is a measure of the asymmetry in the molecular charge distribution and is given as a vector in three dimensions. For Hartree-Fock calculations, this is equivalent to the expectation values of X, Y and Z, which are the quantities reported in the output. The predicted dipole moments (in Debye) at B3LYP level of theory are shown in Table 3. The dipole moment of the molecules gives the strength of the polarity of the molecules. The predicted dipole moment for 3-Chloro Proguanil is less than that of the original molecule at both RHF/(6-31++G & 6-31G(d,p)) B3LYP/(6-31++G & 6-31G(d,p)) level. The molecule is polar and the charge distribution is fairly symmetrical in gas phase. The dipole moments of Proguanil is greater than that of 3-Chloro Proguanil indicating that this molecule is less polar compared to Proguanil.

Table 3 : Dipole moments(in Debye**)**

	RHF		B3LYP/6-31	
Molecule	6-31++G	6-31G(d,p)	6-31++G	6-31G(d,p)
Proguanil (Chifu et al, 2014)	10.1635	-	9.9257	-
Proguanil derivative	7.1033	7.9887	9.0845	7.1576

Quadruapole Moments

Quadrupole moments provide a second order approximation of the total electron distribution, providing at least a crude idea of its shape. One of the components being significantly larger than the others would represent an elongation of the sphere along that axis. If present, the off-axis components represent trans-axial distortion (stretching or compressing of the ellipsoid). The quadrupole moment for the molecule at both DFT and RHF levels of theory is shown in Table 4 and Table 5 below. The molecules are predicted to be slightly elongated more along the ZZ axis in gas phase.

Table 4: RHF obtained Quadrupole moments(in Debye**)**

Molecule	6-31++G			6-31G(d,p)		
	XX	YY	ZZ	XX	YY	ZZ
Proguanil (Chifu et al 2014)	-108.8825	-102.2247	-114.9042	-	-	-
derivative of Proguanil	-97.0849	-106.0731	-113.6536	-101.4627,	-110.0314,	-117.0939

Table 5: B3LYP obtained Quadrupole moments(in Debye**)**

Molecule	6-31++G			6-31G(d,p)		
	XX	YY	ZZ	XX	YY	ZZ
Proguanil (Chifu et al 2014)	-106.2946	-100.7662	-112.2982	-	-	-
Proguanil derivative	-100.9187	-109.6369	-115.7719	-96.5398	-105.4899	-111.1272

Table 6: Predicted total thermal energies (kcal/mol)

Method	RHF		B3LYP	
Molecule	6-31++G	6-31G(d,p)	6-31++G	6-31G(d,p)
Proguanil [4]	195.095	-	182.682	-
2-Chloro-Proguanil	193.332	194.531	182.214	181.439

Polarizability

Polarizability refers to the way the electrons around an atom redistribute themselves in response to an electrical disturbance, dipole polarizability for the molecule are more on XX, YY and ZZ axis as shown in Table 7 below.

Table 7: Polarizabilities of Proguanil derivative

	RHF	B3LYP/6-31G		
orientation	6-31++G	6-31G(d,p)	6-31++G	6-31G(d,p)
XX	-97.0849	-101.4627	-158.6662	-142.6187
XY	15.8708	19.4216	-4.5987	-3.6261
YY	-106.0731	-110.0314	-152.5606	-146.0699
XZ	-0.1113	0.7131	-3.5103	-2.4928
YZ	1.7072	1.4128	1.0933	1.1643
ZZ	-113.6536	-117.0939	-155.4451	-147.5397

3. Vibrational Frequency Analysis

In general, a molecule with N atoms has 3N – 6 normal modes of vibration, but a linear molecule has 3N – 5 such modes, as rotation about its molecular axis cannot be observed. 2-Chloro Proguanil molecule with molecular formula $C_{11}H_{16}N_5Cl$ has a total of 33 atoms and thus N=33; giving 3(33)-6 = 93 possible number of vibrational modes for each IR and Raman frequencies. A vibrational motion for a molecule is when the bonds between atoms within a molecule move. The vibrational coordinate of a normal vibration is a combination of changes in the positions of atoms in the molecule. When the vibration is excited the coordinate changes sinusoidally with a frequency v, the frequency of the vibration. Some of the vibrations observed and their descriptions are as follows:

Table 8: Some IR Intense Vibrational Frequencies and their Approximate Description for 3-Chloro Proguanil at RHF/6-31G(d,p) Level of Theory

S/N	**Frequency**	**Approximate description**
1.	1667.05	Symmetric stretching of NH
2.	1636.83	Symmetric stretching of CH
3.	1952.26	Symmetric stretching of CNH
4.	3255.57	Symmetric stretching of CNH
5.	1667.05	Symmetric stretching of CNH
6.	545.063	Anti symmetric stretching of CNH
7.	1308.38	Bending or Scissoring of the benzyl ring
8.	1165.08	Bending or Scissoring of the molecule

Table 9: Some IR Intense Vibrational Frequencies and their Approximate Description for 3-Chloro Proguanil at RHF/6-31++G Level of Theory

S/N	**Frequency**	**Approximate description**
1.	566.338	Symmetric stretching of NH
2.	802.165	Distortion of the whole molecule
3.	1050.2	Bending or Scissoring HCH
4.	1253.94	Symmetric stretching of CNH
5.	1439.96	bending of CH and NC symmetric stretching
6.	1670.28	Symmetric stretching of CNH and HC bending in the benzyl ring
7.	1714.57	Symmetric stretching of CNH and HC bending in the benzyl ring
8.	1794.29	Distortion of the benzyl ring in the molecule and HN bending
9.	1918.31	Symmetric stretching of NH and bending of HN

Table 10: Some IR Intense Vibrational Frequencies and their Approximate Description for 3-Chloro Proguanil at B3LYP/6-31G(d,p) Level of Theory

S/N	**Frequency**	**Approximate description**
1.	1156.5	Symmetric Stretching of HNC and bending of H in benzyl ring
2.	1336.66	Symmetric Stretching of HNC and bending of H in benzyl ring
3.	1555.12	Symmetric Stretching of the whole molecule
4.	16770.28	Distortion of benzyl ring
5.	1767.72	Symmetric stretching of HCN
6.	3477.36	Symmetric Stretching of HN

Table 11: Some IR Intense Vibrational Frequencies and their Approximate Description for 3-Chloro Proguanil at B3LYP/6-31++G Level of Theory

S/N	**Frequency**	**Approximate description**
1.	1156.50	bending of the CH
2.	1324.80	Anti Symmetric Stretching of HC
3.	1528.54	bending of the CH and bending of H in benzyl ring
4.	1537.40	bending of the CH and H in benzyl ring
5.	1643.70	Distortion of the benzyl ring and breathing of HCN
6.	1750.00	Symmetric Stretching of HNC

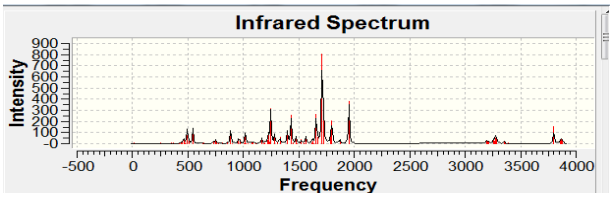

a) 6-31 G(d,p)

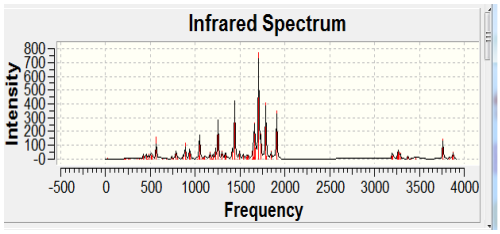

b) 6-31++G

Fig. : IR Spectrum at RHF Level of Theory

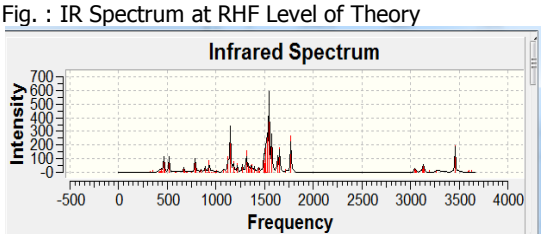

a) 6-31 G(d,p)

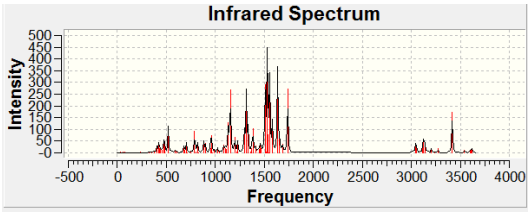

b) 6-31++G

Fig. : IR Spectrum at B3LYP Level of Theory

Table 12: Some Raman Intense Vibrational Frequencies and their Approximate Description for 3-Chloro Proguanil at RHF/6-31G(d,p) Level of Theory

S/N	**Frequency**	**Approximate description**
1.	1026.42	Bending or Scissoring of the HCH
2.	1330.05	Bending or Scissoring of the HCH and HNC
3.	3190.62	H-C Symmetric stretching
4.	3354.47	Symmetric stretching of CH in benzyl ring
5.	3866.02	Symmetric stretching of NH

Table 13: Some Raman Intense Vibrational Frequencies and their Approximate Description for 3-Chloro Proguanil at RHF/6-31++G Level of Theory

S/N	**Frequency**	**Approximate description**
1.	1112.2	Benzyl ring symmetric stretching
2.	1144.29	Benzyl ring distortion
3.	3220. 47	Symmetric stretching of CH
4.	3264.76	Anti symmetric stretching of CNH
5.	3379.92	Symmetric stretching of CH
6.	3902.56	Symmetric stretching of HN
7.	3849.41	Symmetric stretching of NH

Table 14: Some Raman Intense Vibrational Frequencies and their Approximate Description for 3-Chloro Proguanil at RHF/6-31G(d,p) Level of Theory

S/N	**Frequency**	**Approximate description**
1.	1652.56	Distortion of the benzyl ring and breathing of HCN
2.	1767.72	Symmetric stretching of HNC
3.	3061.02	Symmetric stretching of HC
4.	3149.61	Anti Symmetric stretching of HC
5.	3459.65	Symmetric stretching of HN
6.	3592.52	Symmetric stretching of HN

Table 15: Some Raman Intense Vibrational Frequencies and their Approximate Description for 3-Chloro Proguanil at RHF/6-31++G Level of Theory

S/N	**Frequency**	**Approximate description**
1.	1014.76	Distortion of the benzyl ring
2.	1643.70	Bending of benzyl ring and symmetric stretching of HCN
3.	1750.00	Bending of HCN
4.	3069.88	Symmetric stretching of HC
5.	3131.89	Anti Symmetric stretching of HC
6.	3140.75	Anti Symmetric stretching of HC

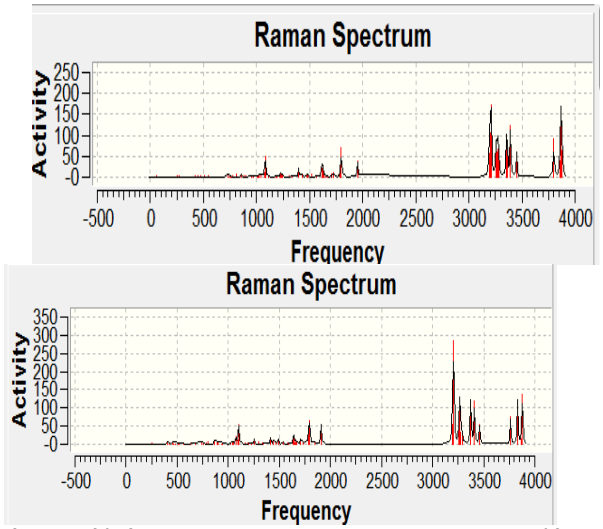

a) 6-31G(d,p) b) 6-31++G

Fig. : Raman Spectrum at RHF Level of Theory

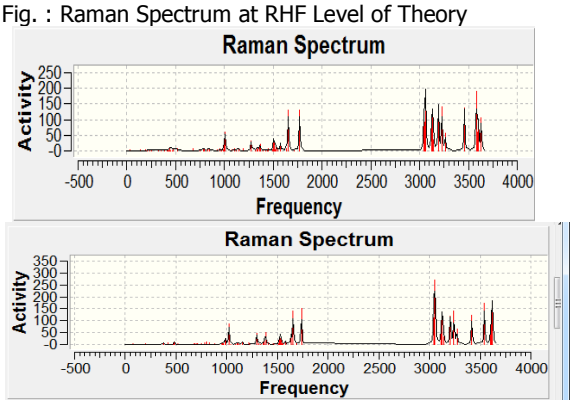

a) 6-31G(d,p) b) 6-31++G

Fig. : Raman Spectrum at B3LYP Level of Theory

CONCLUSION AND RECOMMENDATION

The dipole moment of Proguanil derivative at both levels of theory is less than that obtained for original malaria drug Proguanil. This indicates that Proguanil derivative responds significantly more than Proguanil to an applied electric field. Also, compared to Daraprim, Proguanil has shorter bond lengths and bond angles and higher total energy thus suggesting that the molecule is more stable than Daraprim in gas phase (Geh, 2015). This work provides baseline data for the modeling and subsequent development of future malaria drugs which are derivatives of Proguanil. It is hoped that experimental work will be done in the near future to complement the findings in this work. To compliment this research work, the experimental part of this study can be undertaken to ascertain the accuracy of this computational technique. Also, this work can be done using other computational physics soft-wares and results compared with our results in this work. The studied molecule could be studied in other medium to see the effect of the medium on it is physical properties. Solvents that could be considered include ethanol, hexane, hydronaphthalenes, Carbon disulfide, Chloroform, and other organic solvents.

Acknowledgment

We wish to acknowledge Sule Lamido University Research Committee for providing the funds for this research.

REFERENCES

Becke, A. D. (1988). Density-functional exchange-energy approximation with correct asymptotic behavior, *Physical Review A* **38**: 3098.

Becke A.D. (1993), "Density Functional Thermo chemistry. III. The role of exact exchange", *Journal of Chemical Physics*, 98:5648

Chifu E. Ndikilar, Tasiu Z. and L.S. Taura; *Bayero Journal of Pure and Applied Sciences* , **2014**, 7:(2) 64- 68.

Frisch M J, Trucks G W, Schlegel H B, Scuseria G E, Robb M A, Cheeseman J R, Montgomery J A, Vreven Jr T, Kudin K N, Burant J C, Millam M, Iyengar S S, Tomasi J, Barone V, Mennucci B, Cossi M, Scalmani G, Rega N, Petersson G A, Nakatsuji H, Hada M, Ehara M, Toyota K, Fukuda R, Hasegawa J, Ishida M, Nakajima T, Honda Y, Kitao O, Nakai H, Klene M, Li X, Knox J E, Hratchian H P, Cross J B, Adamo C, Jaramillo J, Gomperts R, Stratmann R E, Yazyev O, Austin AJ, Cammi R, Pomelli C, Ochterski J W, Ayala P Y, Morokuma K, Voth G A, Salvador P, Dannenberg J J, Zakrzewski V G, Dapprich S, Danniels A D, Strain M C, Farkas O, Malick D K, Rabuck A D, Raghavachari K, Foresman J B, Ortiz J V, Cui Q, Baboul A G, Clifford S, Cioslowski J, Stefanov B B, Liu G, Liashenko A, Piskorz P, Komaromi I, Martin R L, Fox D J, Keith T, Al-Laham M A, Peng C Y, Nanayakkara A, Challacombe M, Gill PMW, Johnson B, Chen W, Wong M W, Gonzalez C, and Pople J A, Gaussian, Inc., Wallingford CT, 2004 Gaussian 03, Revision C.02 (2004).

Geh W. Ejuh , S. Nouemo, Chifu E. Ndikilar, F. T. Nya and Njaka J. Marie, *Journal of Advances in Physics* 10(2):2696 - 2714, 2015.

Lee, C., W. Yang, and R. G. Parr, (1988). Development of the Colle-Salvetti correlation-energy formula into a functional of the electron density, *Physical Review* B **37**, 785.

Sachs, J.; Malaney, P. *Nature*, **2002**, *415*, 680-685.

Schwarz, O.; Brun, R.; Bats, J. W.; Schmalz, H-G. *Tetrahedron Lett.*, **2002**, *43*, 1009-1013.

Singh, C.; Srivastav, N. C.; Puri, S. K. *Bioorg. & Med. Chem. Lett.*, **2002**, *12*, 2277-2279.

Snow, R. W.; Guerra, C. A.; Noor, A. M.; Myint, H. Y. *Nature*, **2005**, *434*, 214-217.